Available online at www.sciencedirect.com

ScienceDirect

Procedia Engineering 120 (2015) 427 – 434

Procedia Engineering

www.elsevier.com/locate/procedia

EUROSENSORS 2015

# Polycrystalline NiO nanowires: scalable growth and ethanol sensing

Thi Thanh Le Dang[1,]*, Matteo Tonezzer[2,]†

[a]*ITIMS, Hanoi University of Science and Technology, Hanoi, Viet Nam*
[b]*IMEM-CNR, sede di Trento - FBK, Via alla Cascata 56/C, Povo - Trento, Italy*

**Abstract**

Gas nanosensors are nowadays very important to monitor environment and human conditions in many fields. Low cost synthesis of nanostructured metal oxides is thus crucial to satisfy this need to the best. Herein, nickel oxide p-type semiconducting nanowires with polycrystalline structure were prepared by a facile and scalable hydrothermal method. Morphology and structure of the NiO nanowires were investigated by scan electron microscopy, X-ray diffraction and transmission electron microscopy. The nanostructured materials were then tested as ethanol sensors showing good performance in terms of sensor response, stability, speed and selectivity towards ethanol, ammonia and liquefied petroleum gas.


Peer-review under responsibility of the organizing committee of EUROSENSORS 2015

*Keywords:* gas sensor; ethanol; nickel oxide, nanowires.

## 1. Introduction

Metal oxide semiconductors are very good active materials to be used as sensors. In the last years metal oxide nanostructures replaced thick and thin films in several fields and application, including gas sensing. Semiconducting n-type metal oxides ($SnO_2$ and ZnO among others [1,2]) have been studied more deeply than p-type semiconductors. An extensive study of p-type metal oxides is quite recent, and includes nickel oxide (NiO). Controlling the shape and structure of nanostructures is a common strategy to optimize their performance due to their structure-dependent properties [3-5]. Nanowires are almost one-dimensional (1D) nanostructures, and are ideal elements for functional

* Corresponding author. Tel.: +84-04-3868-0787; fax: +84-04-3869-2963.
*E-mail address:* thanhle@itims.edu.vn
† Corresponding author. Tel.: +39-0461-314-828; fax: +30-0461-314-875.
*E-mail address:* matteo.tonezzer@cnr.it


Peer-review under responsibility of the organizing committee of EUROSENSORS 2015
doi:10.1016/j.proeng.2015.08.658

nanodevices [6]. Nickel oxide, a p-type semiconductor with a band gap energy of about 3.6 - 4.0 eV [7], is being considered as a promising material due to its good chemical stability and electrical properties. Its potential applications cover a wide range of fields: catalysis [8], electrode materials for lithium ion batteries [9], photovoltaic devices [10], fuel cell electrodes, electrochemical supercapacitors [11], electrochromic films [12], magnetic materials [13] and gas sensors [14-16]. Several different NiO nanostructures have been grown up to date, including nanoparticles [17], nanorods [18], nanotubes [19], nanosheets [20]...

Many deposition methods have been used to grow nickel oxide nanostructures, including aqueous solution [21,22], electrochemical deposition [23,24], vapor-based metal etching oxidation method [25], dehydration method [26]. Still, most of the growth techniques used necessitate unfavourable parameters like high vacuum, high temperature and complex chemical reactions, leading to expensive procedures that prevent an extensive use of these materials. The hydrothermal synthetic method here utilized has attracted a broad interest for its simple operation and low power consumption.

In the present work, we investigate the growth of nickel oxalate hydrate ($NiC_2O_4 \bullet 2H_2O$) nanowires via hydrothermal method and their thermal decomposition during calcination at 500°C, thus to obtain polycrystalline nickel oxide nanowires. We study morphology and structure of the nickel oxide nanowires, and use them as gas sensors to quickly and selectively detect ethanol gas.

## 2. Materials and methods

### *2.1. Synthesis of nickel oxide nanowires*

A two-step process consisting in hydrothermal method followed by annealing at 500°C has been used to grow the NiO nanowires. All chemicals used in these experiments were analytical reagent grade and were used without further purification. During a typical procedure, 0.474 g of $NiCl_2.6H_2O$ (Sigma-Aldrich) was dissolved into a mixture of 32 mL ethylene glycol (EG, Sigma-Aldrich) and 18 mL deionized water in a beaker and stirred at room temperature. Then 0.1206 g of $Na_2C_2O_4$ was added, while continuous stirring was carried out to ensure $Ni^{2+}$ ions a homogeneous dispersion in the solution. The solution was then transferred into a teflon-lined stainless steel autoclave, sealed and heated at 200°C for 24 h. At the end of the heating step, the autoclave was let cooling down naturally. The product was collected by centrifugation, rinsed thrice with deionized water and absolute ethanol, respectively, and then dried naturally at room temperature. The resulting product was a blue–green powder consisting of nickel oxalate hydrate ($NiC_2O_4 \cdot 2H_2O$) short nanowires.

The polycrystalline NiO nanowires were obtained by calcination at 500°C of this precursor.

The nickel oxalate hydrate nanowires and the nickel oxide polycrystalline nanowires were characterized by X-ray diffraction (XRD) and scanning electron microscopy (SEM). Calcinated nanowires underwent the same characterizations, including transmission electron microscopy (TEM). The XRD analysis was performed using a Bruker D5005 X-ray diffractometer with CuK$\alpha$1 radiation ($\lambda$=1.5406 Å) operated at 40 kV and 40 mA. SEM characterization was carried out with a JEOL7600 scanning electron microscope at 20 kV. TEM and electron diffraction images were acquired using a JEOL JEM-2100 transmission electron microscope used at 200 kV.

### *2.2. Sensors fabrication*

The sensors were fabricated by drop casting NiO nanowires over interdigitated platinum electrodes on silica substrates. 1 mg of nickel oxide nanowires was dispersed in ethanol and sonicated for 3 minutes. The solution was then dropped onto comb platinum/titanium electrodes on thermally oxidized silicon substrates. The interdigitated contacts were deposited onto $SiO_2$/Si substrates by conventional optical lithography technique and sputtering. The device is 2 mm × 6 mm overall, with two electrodes consisting in 18 pairs of 800 x 20 μm fingers and a gap of 50 μm between fingers. After the drop of nickel oxide nanowires, the sensor was heated up to 500°C in a furnace for 2 h in order to stabilize and improve the adhesion between nanostructures and platinum electrodes.

### *2.3. Gas sensing measurements*

The nickel oxide nanowires-based sensors were tested in dynamic conditions, in which the tested gas and the carrier gas (dry air) were continuously flowing through the test chamber with a total flow of 500 sccm. The sensor testing system was home-built, including a test chamber, a heatable sensor holder and mass flow controllers connected to high purity gas bottles.

The sensors dynamic resistance was measured via a Keithley 2400 multimeter connected to a home-built data acquisition system (LabView, National Instruments). A voltage of 5V was applied to the samples, and they showed a good ohmic behaviour which negligible metal-semiconductor junction resistance. The sensor response S for ethanol (reducing gas) was defined as $S = (R_{GAS} - R_{AIR}) / R_{AIR} \cdot 100$, where $R_{GAS}$ and $R_{AIR}$ are the resistance of the device in presence of ethanol or in pure air, respectively. Response and recovery times are defined as the time needed for the sensors to reach 90% of the maximum response value and to get down to 10% of it, respectively.

## 3. Results and discussion

### *3.1. Nanowires characterization*

Figure 1a shows a SEM image of the material grown during the hydrothermal growth: thin and straight nanowires with a constant diameter around 60 nm and smooth surfaces are visible. The aspect ratio (ratio between length and diameter) of the nanowires depends on the growth temperature, enlarging with increasing temperature. After the calcination at 500°C for 2 hours, the nanowires morphology changes very much, as shown in Figure 1b.

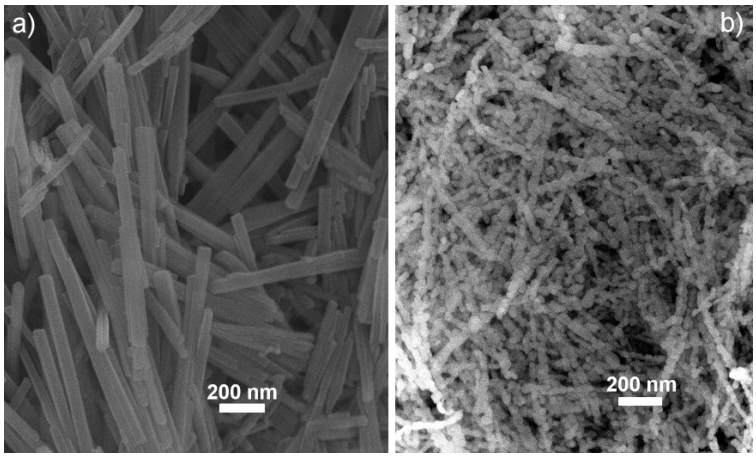


Fig. 1. SEM images of (a) nanowires as hydrothermally grown; (b) nanocrystalline nanowires after calcinations at 500°C.

At such high temperature annealing, the nanowires material agglomerates in many nanoparticles still resembling the former nanowires. The nanoparticles composing each nanowire are roundish with a diameter of about 20-50 nm. X-ray diffraction spectra shown in Figure 2 confirms the composition of the nanostructures before and after the calcination. Figure 2a is relative to the nanowires before calcination, and shows numerous diffraction peaks which can be all assigned to monoclinic nickel oxalate hydrate (JCPDS 25-0581). The XRD spectrum of the nanowires after the calcination process is reported in Figure 2b, showing a well crystallized nickel oxide cubic phase (JCPDS 47-1049). Three intense diffraction peaks are visible at 37.3, 43.4 and 62.9° and can be indexed as cubic NiO, with a lattice parameter of 4.1667 Å.

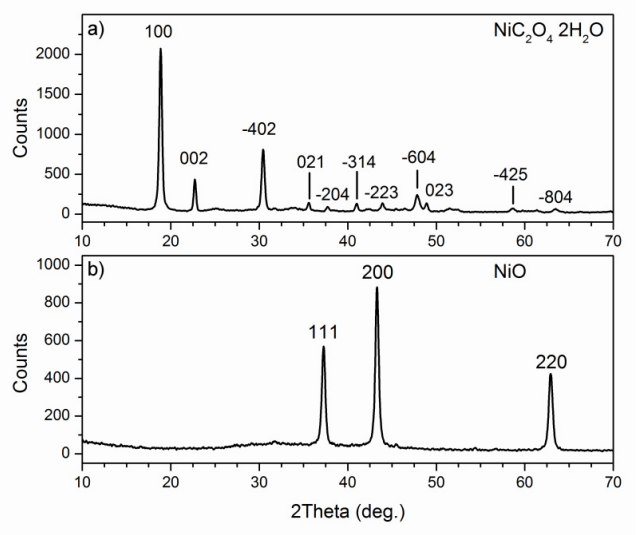


Fig. 2. XRD spectra of (a) nanowires as hydrothermally grown; (b) nanocrystalline nanowires after calcinations at 500°C.

The absence of any impurity phase in both spectra of Figure 2 confirms that the nanowires are completely crystalline before and after the calcination. This means that all the $NiC_2O_4 \bullet 2H_2O$ precursor was converted to NiO during the process.

The crystal structure of the NiO nanowires and the nanoparticles composing them were further characterized by TEM analysis. As shown in Figure 3a, NiO nanowires tend to agglomerate in bundles. The diameter of single nanowire ranges around 40–70 nm, while the whole bundles have diameters around 300-600 nm. Figure 3b shows a high magnification TEM image revealing that the NiO nanoparticles composing the nanowires have diameters around 20–80 nm, with several interspaces between them.

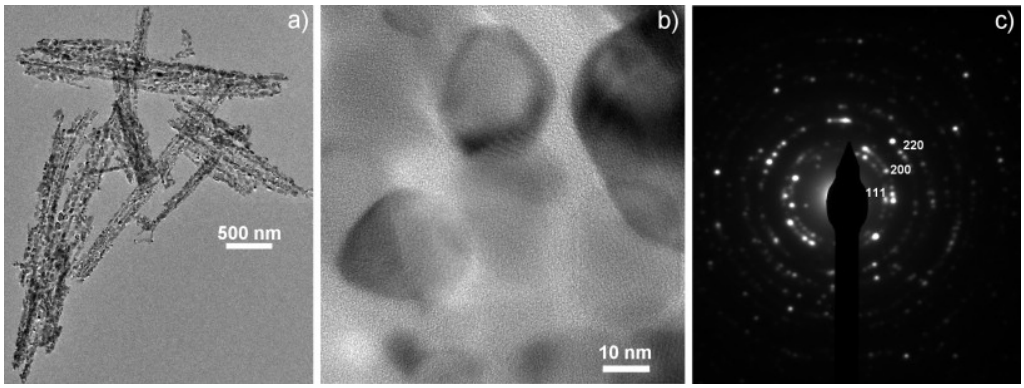


Fig. 3. (a) TEM image of NiO nanowires; (b) HRTEM image of nanoparticles composing a NiO nanowire, (c) SAED pattern of NiO nanowires.

Figure 3b shows lattice fringes spaced of about 0.20 nm, which well agree to the interplanar distance of (200) lattice planes in cubic NiO. Figure 3c shows the selected area electron diffraction pattern of polycrystalline NiO nanowires, with three diffused rings which can be assigned to (111), (200), (220) diffraction lines of cubic NiO phase, respectively.

### 3.2. Gas sensing results

The sensors resistance were tested in the range from -5 V to +5 V and a very good ohmic behaviour was observed. The resistance of the sensors ranged from 43 kΩ to 3.5 MΩ increasing the temperature from 200 to 400°C in air. The nickel oxide devices were tested at a voltage of 5 V between the electrodes, with different gas concentrations and different working temperatures in the apparatus.

Figure 4 presents the sensor resistance as a function of time while different ethanol concentrations (50, 100, 250, 500 and 1000 ppm) where flowing on the device. Each plot is relative to a different working temperature: 200, 250, 300, 350 and 400 °C. The dynamic resistance measured at 200 °C (bottom plot, black line) is noisy and has a small drift. All the other plots show a stable resistance of the NiO nanowires in air, which abruptly increases when ethanol gas is injected into the testing system. Once the ethanol flow is stopped and replaced with dry air, the device resistance quickly decreases to its previous value.

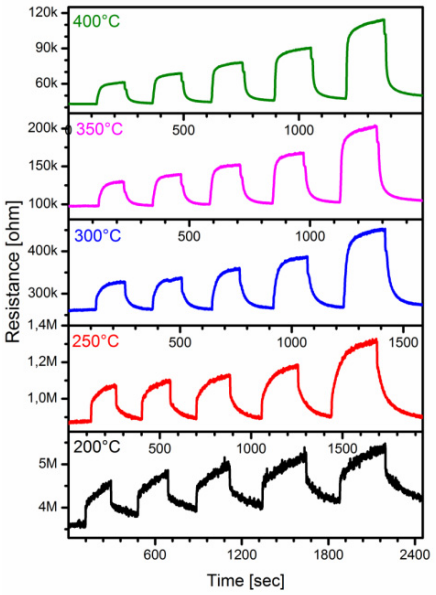


Fig. 4. Dynamic resistance of a sensor under different ethanol concentrations (50, 100, 250, 500 and 1000 ppm) at 200 – 400°C.

This is the typical response of p-type semiconductor sensors. Nickel oxide is commonly a p-type semiconductor, using holes as charge carriers. While the NiO nanograins are exposed to air, oxygen molecules in the form of $O^-$ and $O^{2-}$ are absorbed on their surface. The reaction of adsorbed oxygen with the surface atoms withdraws electrons from the nanowire, increasing the number of electrical holes, thus augmenting its conductivity in these conditions. Once a reductive gas like ethanol is injected in the system, its molecules react with the adsorbed oxygen, releasing the electrons back to the nanowires. This results in a decrease of holes and a shrink of the sensor conductance.

As can be seen in Figure 4, the response intensity of the sensor improves while increasing ethanol concentration at all operating temperatures. The sensor response is always sharp and clear, and the recovery is very good with negligible drifts (except at 200°C).

The response as a function of the ethanol concentration is calculated from Figure 4 and reported in Figure 5a. I can be seen that at every working temperature the sensor response raises with increasing gas concentration, with a slope that slowly decreases at high concentrations. In the range 100 - 1000 ppm the response increases linearly, meaning that the nanowires are not saturating yet. This indicates that the sensors could be used in a wide range of ethanol concentrations. The lowest sensor response of NiO nanowires based sensors goes from 20.0% to 24.1% at 200°C. The best values go from 42.1% to 140.0% at 400°C.

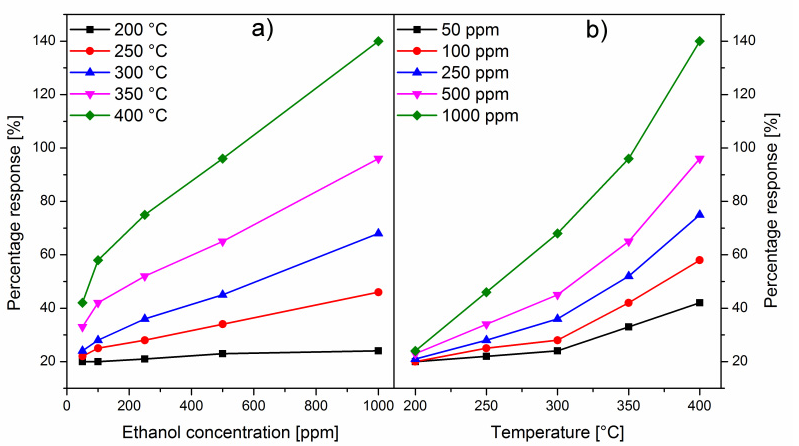


Fig. 5. Percentage response as a function of (a) ethanol concentration and (b) working temperature.

Figure 4b reports a plot of the response values towards the working temperature, showing that the sensor responds better at higher temperatures. The higher the working temperature, the better the sensor response, at all ethanol concentrations. We didn't increase further the working temperature because -of limitations of our experimental setup, but also because it is difficult to operate devices at higher temperatures in real applications.

Figure 6 shows the speed of a sensor responding to and recovering from different ethanol concentrations at diverse working temperatures. Response times are reported in Figure 6a, while recovery times are shown in Figure 6b. Response and recovery times show very similar behaviors with both gas concentration and working temperature. In the 300 - 400°C temperature range there is no evident dependency on the ethanol concentration, while at lower working temperatures the device seems to respond and recover more slowly to higher ethanol concentrations. The response time ranges 150 - 210 seconds at 200°C, 45 - 55 seconds at 300°C and 30 - 43 seconds at 400°C. The recovery times shown in Figure 6b are slightly lower: 93 - 176 seconds at 200°C, 43 - 59 seconds at 300 °C and 34 - 39 seconds at 400°C.

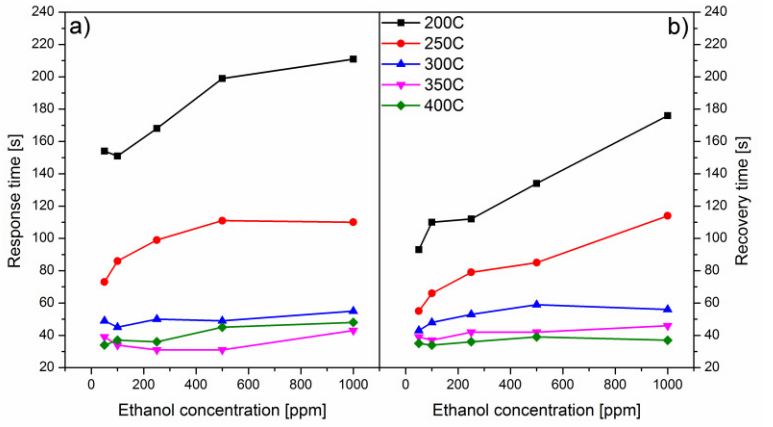


Fig. 6. (a) Response times and (b) recovery times as a function of ethanol concentration at different working temperatures.

We have also calculated limit of detection (LoD), the lowest gas concentration that the device can sense. A linear fit of the sensor response at low gas concentration has been used, as long as three times the standard deviation of the base signal. As can be seen in Figure 7a, the limit of detection is good at 200°C with a value of 2.2 ppm, and decreases at higher working temperatures, reaching the best value of 200 ppb at 400 °C. The capability of detecting

a very low gas concentration is an important characteristic for a sensor to be used in applications where a low threshold is required.

Selectivity of the NiO nanowires has been studied towards hydrogen, ammonia ($NH_3$) and liquified petroleum gas (LPG). The response values of the NiO nanowires-based sensors to 100 ppm of different gases (while working at 400 °C) are presented as a polar plot in Figure 7b. The high directionality of the green shape in Figure 8 demonstrates the good selectivity of the device to ethanol while compared to hydrogen, $NH_3$ and LPG. At a working temperature of 400°C, the NiO sensor gives a response of around 59% to ethanol, while the response to hydrogen, $NH_3$ and LPG is 24.1%, 15.9 and 4.8%, respectively. This demonstrates that the NiO polycrystalline nanowires can be used as fast and selective ethanol sensors.

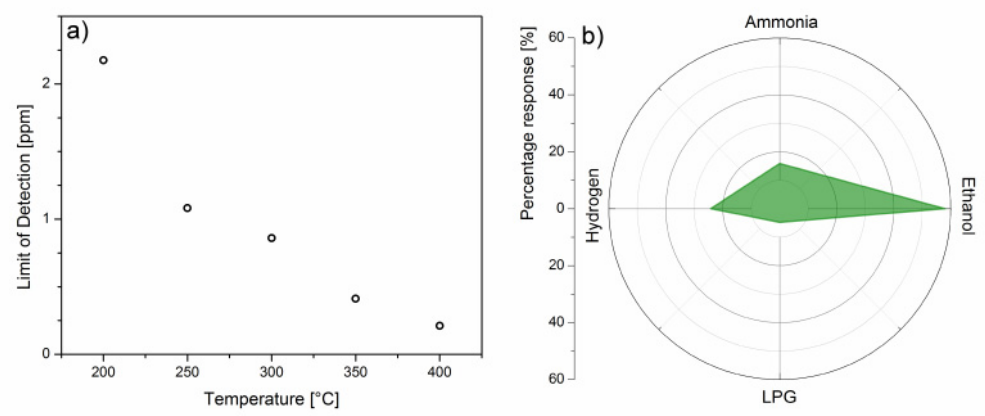


Fig. 7. (a) Limit of detection as a function of the sensor working temperature and (b) selectivity plot at 200°C for 100 ppm of gas.

## 4. Conclusions

NiO polycrystalline nanowires have been grown through a simple and cheap two-step process consisting in hydrothermal growth followed by calcination. The resulting polycrystalline nanowires, composed by NiO nanoparticles, show very good ethanol sensing properties with response values reaching 140%, quick response and recovery (down to few tens of seconds) and good selectivity to ethanol towards ammonia, hydrogen and liquefied petroleum gas.

## Acknowledgements

This research is funded by Vietnam National Foundation for Science and Technology Development (NAFOSTED) under grant number **103.02-2013.23**, and by the Italian Ministry of Foreign Affairs and International Cooperation (MAECI) with the bilateral project HyMN. Authors acknowledge to Laboratory of Geology, Geoengineering, Geoenvironment and Climate Change at Vietnam National University, Hanoi for HRTEM characterizations.

## References

[1] M.F. Bianchetti, C. Arrieta, N.E. Walsoee de Reca, Microstructural study of nanocrystalline pure and doped tin dioxide to be used for resistive gas sensors, Sens. Actuators B 217 (2015) 113–118.

[2] M. Tonezzer, S. Iannotta, Zinc oxide porous nanohexagones: $H_2$ sensing properties of 2D nanostructures, Talanta 122 (2014) 201–208.

[3] M. Tonezzer, N.V. Hieu, Size-dependent response of single-nanowire gas sensors, Sens. Actuators B 163 (2012) 146–152.
[4] Byung-Yong Wang, Dae-Soon Lim, and Young-Jei Oh, CO Gas Detection of Al-Doped ZnO Nanostructures with Various Shapes, Jpn. J. Appl. Phys. 52 (2013) 101103.
[5] Matteo Tonezzer, Le Thi Thanh Dang, Nicola Bazzanella, Van Hieu Nguyen and Salvatore Iannotta, Comparative gas-sensing performance of 1D and 2D ZnO nanostructures, Sens. Actuators B 220 (2015) 1152–1160.
[6] André Heinzig, Thomas Mikolajick, Jens Trommer, Daniel Grimm and Walter M. Weber, Dually Active Silicon Nanowire Transistors and Circuits with Equal Electron and Hole Transport, Nano Lett. 13 (2013) 4176–4181.
[7] Raffaella Lo Nigro, Sergio Battiato, Giuseppe Greco, Patrick Fiorenza, Fabrizio Roccaforte, Graziella Malandrino, Metal Organic Chemical Vapor Deposition of nickel oxide thin films for wide band gap device technology, Thin Solid Films 563 (2014) 50-55.
[8] Manohar A. Bhosale, Bhalchandra M. Bhanage, Rapid synthesis of nickel oxide nanorods and its applications in catalysis, Adv. Powder Technol. 26 (2015) 422-427.
[9] B. Varghese, M.V. Reddy, Z.Y. Wu, C.S. Lit, T.C. Hoong, Fabrication of NiO nanowall electrodes for high performance lithium ion battery, Chem. Mater. 20(2008) 3360–3367.
[10] Kuo-Chin Wang, Jun-Yuan Jeng, Po-Shen Shen, Yu-Cheng Chang, Eric Wei-Guang Diau, Cheng-Hung Tsai, Tzu-Yang Chao, Hsu-Cheng Hsu, Pei-Ying Lin, Peter Chen, Tzung-Fang Guo & Ten-Chin Wen, p-type Mesoscopic Nickel Oxide/Organometallic Perovskite Heterojunction Solar Cells, Scientific Reports 4 (2014) 4756.
[11] Mei Zhou, Yafeng Deng, Kun Liang, Xiaojiang Liu, Bingqing Wei, Wencheng Hu, One-step route synthesis of active carbon@La2NiO4/NiO hybrid coatings as supercapacitor electrode materials: Significant improvements in electrochemical performance, J. Electroanal. Chem. 742 (2015) 1-7.
[12] Jessica Denayer, Geoffroy Bister, Priscilla Simonis, Pierre Colson, Anthony Maho, Philippe Aubry, Bénédicte Vertruyen, Catherine Henrist, Véronique Lardot, Francis Cambier, Rudi Cloots, Surfactant-assisted ultrasonic spray pyrolysis of nickel oxide and lithium-doped nickel oxide thin films, toward electrochromic applications, Appl. Surf. Sci. 321 (2014) 61-69.
[13] S.D. Tiwari, K.P. Rajeev, Magnetic properties of NiO nanoparticles, Thin Solid Films 505(2006) 113–117.
[14] J.A. Dirksen, K. Duval, T.A. Ring, NiO thin-film formaldehyde gas sensor, Sens. Actuators B 80(2001) 106–115.
[15] C.Y. Lee, C.M. Chiang, Y.H. Wang, R.H. Ma, A self-heating gas sensor with integrated NiO thin-film for formaldehyde detection, Sens. Actuators B 122(2007) 503–510.
[16] C. Luyo, R. Ionescu, L.F. Reyes, Z. Topalian, Gas sensing response of NiO nanoparticle films made by reactive gas deposition, Sens. Actuators B 138(2009) 14–20.
[17] E.R. Beach, K. Shqau, S.E. Brown, S.J. Rozeveld, P.A. Morris, Solvothermal synthesis of crystalline nickel oxide nanoparticles, Mater. Chem. Phys. 115(2009) 371–377.
[18] N. Srivastava, P.C. Srivastava, Synthesis and characterization of (single- and poly-) crystalline NiO nanorods by a simple chemical route, Physica E 42(2010) 2225–2230.
[19] S.A. Needham, G.X. Wang, H.K. Liu, Synthesis of NiO nanotubes for use as negative electrodes in lithium ion batteries, J. Power Sources 159 (2006) 254–257.
[20] Z.H. Liang, Y.J. Zhu, X.L. Hu, β-Nickel Hydroxide Nanosheets and Their Thermal Decomposition to Nickel Oxide Nanosheets, J. Phys. Chem. B 108(2004) 3488–3491.
[21] Y. Zhan, C. Zheng, Y. Liu, G. Wang, Synthesis of NiO nanowires by an oxidation route, Mater. Lett. 57(2003) 3265–3268.
[22] L. Wu, Y. Wu, H. Wei, Y. Shi, C. Hu, Synthesis and characteristics of NiO nanowire by a solution method, Mater. Lett. 58(2004) 2700–2703.
[23] Y. Lin, T. Xie, B. Cheng, B. Geng, L. Zhang, Ordered nickel oxide nanowire arrays and their optical absorption properties, Chem. Phys. Lett. 380(2003) 521–525.
[24] K. Nielsch, F. Müller, A. Li, U. Gösele, Uniform Nickel Deposition into Ordered Alumina Pores by Pulsed Electrodeposition, Adv. Mater. 12(2000) 582–586.
[25] Z.P. Wei, M. Arredondo, H.Y. Peng, Z. Zhang, D.L. Guo, G.Z. Xing, Y.F. Li, L.M. Wong, S.J. Wang, N. Valanoor, T. Wu, A template and catalyst-free metal-etching-oxidation method to synthesize aligned oxide nanowire arrays: NiO as an example, ACS Nano 4(2010) 4785–4791.
[26] H. Pang, Q. Lu, Y. Zhang, Y. Li, F. Gao, Selective synthesis of nickel oxide nanowires and length effect on their electrochemical properties, Nanoscale 2(2010) 920–922.